# Extensions of Dirac Chord Method with Quasi-Probability Distributions

Alexander Yu. Vlasov

December 2010

**Abstract**

Dirac chord method may be used in many areas of physics for calculation of specific six-dimensional integrals for a convex body using probability density of chord length distribution. Attempts to apply similar methods for nonconvex bodies in some cases may produce instead of probability density some function with negative values. In the work is discussed interpretation of such a function using alternating sums of probability distributions. It is also shown an agreement of such construction with an alternative definition via second derivative of autocorrelation function. It is discussed application of such quasi-probability distributions for Monte Carlo calculations of some integrals for single body of arbitrary shape and for systems with two or more objects.

## 1 Introduction

Let us consider an integral

$$\mathfrak{F}_{B_1}^{B_2}(\varphi) = \int_{B_2}\int_{B_1} \frac{\varphi(|\mathbf{r}_1 - \mathbf{r}_2|)}{4\pi|\mathbf{r}_1 - \mathbf{r}_2|^2} d\mathbf{V}_1 d\mathbf{V}_2, \tag{1}$$

there $B_1$ and $B_2$ — are three-dimensional bodies, vectors $\mathbf{r}_1 = (x_1, y_1, z_1) \in B_1$ and $\mathbf{r}_2 = (x_2, y_2, z_2) \in B_2$ represent pair of points, $d\mathbf{V}_1 = dx_1 dy_1 dz_1$ and $d\mathbf{V}_2 = dx_2 dy_2 dz_2$.

Similar integrals are used in many different physical applications, *e.g* for calculations based on *point-kernel* method in radiation shielding and dosimetry [1, 2].

If $B_1 = B_2 = B$ — is the same *convex* body, the *Dirac chord method* [3] may be applied for calculation of the particular case of the double integral Eq. (1) over pairs of points in the convex body $B$ using probability density of chord lengths distribution, $\mu(l)$

$$\mathfrak{D}_B(\varphi) = \int_B\int_B \frac{\varphi(|\mathbf{r}_1 - \mathbf{r}_2|)}{4\pi|\mathbf{r}_1 - \mathbf{r}_2|^2} d\mathbf{V}_1 d\mathbf{V}_2 = \frac{S_B}{4}\int_0^\infty \mu(l)\Big(\int_0^l\int_0^r \varphi(x)dx\,dr\Big)dl. \tag{2}$$

Here vectors $\mathbf{r}_1$, $\mathbf{r}_2 \in B$ represent pair of points of the body $B$ and $S_B$ is the surface area of $B$. The infinite upper limit of integration is used in the right-hand side of Eq. (2) and many similar equations below, because $\mu(l) = 0$ for $l > l_{\max}$, there $l_{\max}$ is maximal possible length of a chord.

Such a formula may be used in analytical and numerical methods of the calculation of the integrals like $\mathfrak{D}_B(\varphi)$. The most obvious advantage is reduction of six-dimensional integration to simpler expressions like Eq. (2). It is possible to obtain direct analytical expressions for chord length distribution (CLD) for some shapes and it was initially used by Dirac *et al* [4].

Analytical expressions may be found only for few simple shapes and it is reasonable to consider application of Eq. (2) for numerical calculations of integrals, *e.g.*, for Monte Carlo methods [5]. It is indeed very promising and briefly discussed below. For application of Monte Carlo methods here is also important possibility to get rid of singularity $1/R^2$ in left-hand side of Eq. (2), and it may be also actual for Eq. (1) with two neighboring or intersecting bodies $B_1$ and $B_2$.

However, even generalization of Eq. (2) for single *nonconvex* body is not unique, because straight line may intersect such body more than one time and appropriate choice of definition of CLD is not quite clear in such a case.

There are three different and widely used definitions of CLD for nonconvex body [6, 7, 8, 9, 10, 11, 12, 13]. We may consider all intervals of the same line inside of nonconvex body as separate chords and produce *multi-chord distribution* (MCD). It is also possible to calculate sum of lengths of all such intervals to define *one-chord distribution* (OCD).

The third definition introduces "generalized chord distribution" via second derivative of autocorrelation function divided on some normalizer (*e.g.*, $S_B/4$) [9, 10, 12, 14]. It is justified, because for a convex body such a formal expression is equal to probability density for CLD. In more general case such a definition is also useful, because it ensures validity of Eq. (2) [15] and it is discussed below. However, for nonconvex bodies such function may be negative for some arguments [11, 12].

In presented paper are utilized methods of construction of such functions as a sum of some probability densities alternating in signs. Such approach let use direct analogue of Eq. (2) for calculation of integrals for *nonconvex bodies* [15]. Extensions of this techniques [16] may be used also for treatment of more difficult case Eq. (1) with two different bodies.

**Plan of the paper.** In Sec. 2 is revisited a *ray method* as a facilitated analogue of the Dirac chord method. It produces an understanding physical model and introduces simplified versions of some tools applied further for chords. In Sec. 3 are collected some equations useful further for discussion about applications of chord method in Sec. 4. Applications for the Eq. (1) with two bodies and multi-body case are discussed in Sec. 5. Methods of applications of considered techniques for statistical (Monte Carlo) sampling are discussed mainly in Sec. 2.2, Sec. 4.2, and Sec. 5.3, Sec. 5.4.

## 2 Ray method

### 2.1 Ray length distribution

There is analog of Eq. (2) with probability density of ray length distribution (RLD), $\iota(l)$, *i.e.* instead of full chord is considered only segment of straight line drawn from given point inside body to surface. It may be written in such a case

$$\mathfrak{D}_B(\varphi) = V_B \int_0^\infty \iota(l)\Big(\int_0^l \varphi(x)dx\Big)dl, \tag{3}$$

there $V_B$ is volume of B. This expression could be considered as intermediate step in derivation of Eq. (2) in [3] and may be simpler for explanation.

Let us introduce simple isotropic homogeneous model with particles emitted inside a convex body $B$ and traveling along straight lines. If absorption of energy on distance $l$ from source is defined by $\varphi(l)$, the left-hand side of Eq. (2) or Eq. (3) with six-dimensional integral describes fraction of energy absorbed inside of the body.

On the other hand, the same value may be calculated using distribution of particle tracks (rays) inside body. The part of energy, absorbed on a ray with length $l$ is

$$I_\varphi(l) = \int_0^l \varphi(x)dx \tag{4}$$

and fraction of rays with length $l$ is described by RLD $\iota(l)$. Taking into account total amount of emitted particles proportional to volume of $B$ we conclude informal visual explanation of Eq. (3).

The example with rays is also useful for explanation of appearance of alternating sum of distributions. Let us consider example with nonconvex body and a ray with three intersections with the boundary Fig. 1.

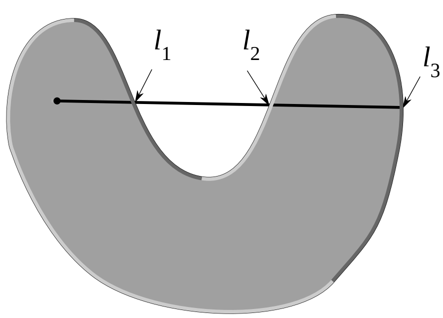


Figure 1: Ray in nonconvex body

For each such ray instead of Eq. (4) for calculation of energy absorbed *inside* of the nonconvex body should be used expression

$$\int_0^{l_1} \varphi(x)dx + \int_{l_2}^{l_3} \varphi(x)dx = I_\varphi(l_1) - I_\varphi(l_2) + I_\varphi(l_3), \tag{5}$$

were $I_\varphi$ is antiderivative of $\varphi$, defined by Eq. (4). It is possible to introduce three (or more) distributions $\iota_k$ (of distances from the source to $k$-th intersection) and write instead of Eq. (3)

$$\begin{aligned} \mathfrak{D}_B(\varphi) &= V_B \sum_{k=1}^{k_{\max}} (-1)^{k+1} \int_0^\infty \iota_k(l) \Big( \int_0^l \varphi(x)dx \Big) dl \\ &= V_B \int_0^\infty \Big[ \sum_{k=1}^{k_{\max}} (-1)^{k+1} \iota_k(l) \Big] \Big( \int_0^l \varphi(x)dx \Big) dl, \end{aligned} \tag{6}$$

there $k_{\max}$ is the maximal number of intersections of a ray with the boundary of $B$. The alternating sum in square brackets in Eq. (6) may be considered as a "quasi-probability distribution" $\tilde{\iota}(l)$ and it let us write an analogue of Eq. (3)

$$\mathfrak{D}_B(\varphi) = V_B \int_0^\infty \tilde{\iota}(l) \Big( \int_0^l \varphi(x)dx \Big) dl, \quad \tilde{\iota}(l) = \sum_{k=1}^{k_{\max}} (-1)^{k+1} \iota_k(l). \tag{7}$$

More rigorous treatment may use so-called *signed measures (charges)* [17] instead of term *quasi-probability distribution* used here. Some details may be found in [15].

The visual derivation of equations with rays in this section is rather informal. It was used understanding description with particles propagated along straight lines. Such a model may create a wrong impression about impossibility to apply such methods to more difficult models with scattering. It is not so, because the only essential condition is the possibility to use in integrals like Eq. (2) expressions depending merely on $|\mathbf{r}_1 - \mathbf{r}_2|$.

An example of appropriate model is convex body and absence of the scattering, but yet another case is an arbitrary body inside of the medium with the same properties. Last example ensures possibility to apply Eq. (2), Eq. (3) and further generalizations to expressions with so-called *buildup factors* used in dosimetry and radiation shielding to take into account scattering [1, 2]. For homogeneous and isotropic case such buildup factors (for given energy) are again depending only on distance from point source.

To make consideration more rigor [3] let us introduce polar coordinates in the second integral Eq. (2) and for convex body it is possible to write

$$\mathfrak{D}_B(\varphi) = \int_B d\mathbf{V}_1 \int_0^\pi \sin\theta d\theta \int_0^{2\pi} d\phi \int_0^{l(\mathbf{r}_1,\theta,\phi)} \frac{\varphi(R)}{4\pi} dR, \tag{8}$$

there $R = |\mathbf{r}_1 - \mathbf{r}_2|$, together with $\theta, \phi$ are polar coordinates of vector $\mathbf{R} = \mathbf{r}_2 - \mathbf{r}_1$ and $l(\mathbf{r}_1, \theta, \phi)$ is length of ray from point $\mathbf{r}_1$ with direction given by polar angles $\theta$ and $\phi$.

The notation $d\mathbf{\Omega} = \sin\theta\, d\theta\, d\phi$ for the invariant measure on surface of unit sphere $\mathbf{S}$ may be used for simplification

$$\mathfrak{D}_B(\varphi) = \int_B d\mathbf{V}_1 \int_{\mathbf{S}} \frac{d\mathbf{\Omega}}{4\pi} \int_0^{l(\mathbf{r}_1,\mathbf{\Omega})} \varphi(R) dR, \tag{9}$$

where $l(\mathbf{r}_1, \mathbf{\Omega})$ is length of a ray from given point $\mathbf{r}_1$ with given direction $\mathbf{\Omega}$ (denoted earlier as $\theta$, $\phi$).

Now Eq. (3) may be derived, if to take into account normalizing multipliers $V_B$ (volume of body $B$) and $4\pi$ (area of surface of unit sphere). It is explained below in Sec. 3. Some additional technical discussion and references may be also found in [15]. Here is important to emphasize that ray in Eq. (9) is not necessary a particle trajectory, but formal integration on variable $R$ along an "axis" $\mathbf{R}$.

Moreover, the formulas with integrations on few disjoint intervals for nonconvex body like Eq. (5) or Eq. (6) are also appropriate here and so Eq. (7) is valid. It is now possible to use that also for arbitrary homogeneous and isotropic case, *i.e.*, for models with scattering.

The important example is a body (convex or nonconvex) inside of environment with identical or similar properties. In such a case the term in left-hand side of Eq. (2) depends only on distance $|\mathbf{r}_1 - \mathbf{r}_2|$ even for points $\mathbf{r}_2$ near boundary. For convex body with straight tracks it is also true, but the environment does not matter, because trajectories of particles between two points inside of the body may not intersect environment unlike the case with scattering.

## 2.2 Method Monte Carlo with rays

A useful application of Eq. (2) and Eq. (3) is Monte Carlo calculation of the integrals. There is additional advantage for the calculation of such integrals with many different $\varphi(l)$ for each body. In such a case CLD or RLD for given body is calculated only once and used further with different functions $\varphi(l)$. Functions, expressed via the definite integrals (single or double) of $\varphi(l)$ in right-hand side of the equations may be calculated either numerically or analytically.

Monte Carlo sampling of a distribution is a standard procedure and may be visually represented as some *histogram.* Interval between zero and maximal possible length is divided on $n$ *bins*, *i.e.* intervals $l_j < l \le l_j + \Delta l$, $j = 0, \ldots, n-1$ and during simulation for each step number of "hits" in appropriate bin is increased by one. For equal bins the number $j$ is simply integer part of $l/n$ and tracing of such data in Monte Carlo simulations is fairly fast and useful procedure.

For application of Eq. (7) it is possible instead of construction $k_{\max}$ different distributions to directly create $\tilde{\iota}$ at once. If a ray intersects boundary in few points it is necessary to consider intervals from origin to all points of intersection. For length of each interval with odd index (first, second, *etc.*) it is necessary to add unit to number of hits in a bin, but for interval with even index it is necessary to subtract unit from a number in relevant bin.

Such a method describes Monte Carlo algorithm for generation of function $\tilde{\iota}(l)$. More difficult algorithms for quasi-probability distributions of chords is discussed below. However, it is reasonable at first to discuss some methods for explanation, why such algorithms are relevant with alternative definitions via derivatives of autocorrelation function.

## 3 Helpful analytical equations

There are few functions related with presented models. It was already mentioned the chord length (distribution) density $\mu(l)$, the ray length (distribution) density $\iota(l)$, and autocorrelation function, denoted further as $\gamma(l)$. It is also convenient to consider probability density of the distances distribution (DD) $\eta(l)$. There are important relations between these functions [6, 7, 8, 9, 10, 12, 14, 15, 18, 19]

$$\mu(l) = \frac{\bar{l}}{V_B}\gamma''(l), \tag{10}$$

$$\mu(l) = -\bar{l}\,\iota'(l) \tag{11}$$

$$\iota(l) = -\frac{1}{V_B}\gamma'(l), \tag{12}$$

$$\eta(l) = \frac{4\pi l^2}{V_B^2}\gamma(l), \tag{13}$$

where $V_B$ is volume of body $B$ and $\bar{l} = \int_0^\infty l\,\mu(l)dl$ is average chord length, that may be simply found for convex body due to widely used Cauchy relationship [3, 18, 20, 21, 22]

$$\bar{l} = 4\frac{V_B}{S_B}. \tag{14}$$

Autocorrelation function $\gamma(l)$ is defined here for body with density $\rho(\mathbf{r}) = 1$ for $\mathbf{r} \in B$ as

$$\gamma(\mathbf{r}) = \int_B \rho(\mathbf{r_1})\rho(\mathbf{r_1}+\mathbf{r})d\mathbf{V}_1, \quad \gamma(l) = \frac{1}{4\pi l^2}\int_{|\mathbf{r}|=l}\gamma(\mathbf{r})d\mathbf{\Omega}, \tag{15}$$

*i.e.* $d\mathbf{V}_1 = dx_1dy_1dz_1$, $\mathbf{r}_1 = (x_1, y_1, z_1)$ and $\gamma(l)$ is an average of $\gamma(\mathbf{r})$ on a sphere with radius $l$. Definition of $\gamma$ here is lack of $1/V_B$ multiplier in comparison with other works [15] and it causes insignificant difference in few equations. In fact, further is only used property Eq. (13) for $\gamma(l)$ and so formal definition Eq. (15) is presented for completeness.

Distances distribution $\eta(l)$ is simply defined for convex, nonconvex body and also for system of two bodies. For explanation of relations between derivatives of $\gamma$ in Eq. (10) and Eq. (12) it is convenient to start with expression

$$\frac{1}{V_B^2}\mathfrak{D}_B(\varphi) = \frac{1}{V_B^2}\int_B\int_B \frac{\varphi(|\mathbf{r}_1-\mathbf{r}_2|)}{4\pi|\mathbf{r}_1-\mathbf{r}_2|^2}d\mathbf{V}_1 d\mathbf{V}_2 = \int_0^\infty \frac{\varphi(l)}{4\pi l^2}\,\eta(l)dl. \tag{16}$$

It may be explained using some methods of probability theory appropriate here due to discussion on statistical sampling methods. Left-hand side of Eq. (16)

may be considered as average of some function $\Phi(R) = \varphi(R)/(4\pi R^2)$ of a variable $R = |\mathbf{r}_1 - \mathbf{r}_2|$ defined on space $B \times B$.

The multiplier $V_B^2$ is measure ("6D volume") of this six-dimensional space $B \times B$ and division on this value follows from standard definition of averaging. On the other hand, due to standard relation of an average ($\mathbf{E}$) with mathematical expectation [23]

$$\mathbf{E}\Phi(R) = \int \Phi(l)\, d_l F_R(l), \tag{17}$$

where $F_R(l)$ is (cumulative) distribution function of random variable $R$ and $d_l F_R(l)$ denotes probability density of $R$, but it is just DD density defined earlier $\eta(l)dl = d_l F_R(l)$, because $R$ is distance between points and double integral (averaging) corresponds to homogeneous distribution of such points.

Due to relation Eq. (13) it is possible to rewrite Eq. (16)

$$\mathfrak{D}_B(\varphi) = \int_0^\infty \varphi(l)\, \gamma(l) dl. \tag{18}$$

After integration by parts it is possible to rewrite Eq. (18)

$$\mathfrak{D}_B(\varphi) = \int_0^\infty [-\gamma'(l)] \Big( \int_0^l \varphi(x) dx \Big) dl. \tag{19}$$

For a convex body Eq. (19) is in agreement with Eq. (3) and Eq. (12).

Really, Eq. (3) also may be proven using analogue of statistical approach discussed above. A proof may be found elsewhere [15] and only briefly sketched here. It is possible to consider Eq. (9) as averaging on five-dimensional space of rays, represented as product $B \times \mathbf{S}$ of body $B$ on unit sphere $\mathbf{S}$. It is necessary to use for normalization volume $V_B$ of $B$ multiplied on surface of unit sphere $4\pi$. In such a case Eq. (3) may be considered as an analogue of Eq. (17) for mathematical expectation of some function depending on length of ray.

It is possible to derive equivalent of Eq. (12) for *nonconvex body* with $\tilde{\imath}(l)$ introduced in Eq. (7) if to use generalized functions and derivatives. The idea of generalized function is convenient for further work with integrals like $\mathfrak{D}(\varphi)$.

The *generalized function* may be defined [17] as a *continuous linear functional* $\mathfrak{T}(\phi)$ on a space of a *test functions* $\phi$. Usual integrable function $\psi$ may be associated with the functional $\mathfrak{T}_\psi$ defined for a test function $\phi(x)$ as

$$\mathfrak{T}_\psi(\phi) = \int_{-\infty}^\infty \psi(x)\phi(x) dx. \tag{20}$$

On the other hand the $\mathfrak{D}_B : \varphi \to \mathfrak{D}_B(\varphi)$ is also linear functional on test functions $\varphi$ and may be considered as some generalized function on $(0, \infty)$, defined by given body $B$. The topology on space of test functions and continuity, *i.e.*, $\mathfrak{D}_B(\varphi_k) \to \mathfrak{D}_B(\varphi)$ for $\varphi_k \to \varphi$ [17] are not discussed here.

It is often used simplified notation $\psi$ instead of $\mathfrak{T}_\psi$ for such a *regular* generalized function defined by Eq. (20) [17]. In such a case Eq. (18) may be rewritten as $\mathfrak{D}_B = \gamma$.

The *generalized derivative* [17] is defined as functional

$$\mathfrak{T}'(\phi) = -\mathfrak{T}(\phi'). \tag{21}$$

Due to Eq. (3) it is possible for convex body $B$ to write $\mathfrak{D}'_B = -V_B\,\iota$ and Eq. (7) for arbitrary body ensures $\mathfrak{D}'_B = -V_B\,\tilde{\iota}$.

# 4 Chord method

## 4.1 Chord length distribution

For convex body Eq. (2) may be rewritten with generalized functions and derivatives as $\mathfrak{D}''_B = (S_B/4)\mu$. Here generalized functions may be more appropriate, because due to the expression with second derivative CLD is not a regular function already if DD continuous, but non-smooth in some points.

Formally, for convex body expression with additional integration along a chord appears due to rearrangement of integral Eq. (8) and consideration of all possible rays with origins along the same chord Fig. 2 [3].

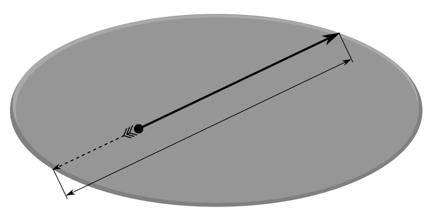

Figure 2: Consideration of all possible rays along a chord

If to use compact notation $\int d\mathcal{L}$ for formal integration on four-dimensional space of straight lines [20, 21], it is possible to rewrite Eq. (9) after such rearrangement as

$$\mathfrak{D}_B(\varphi) = \int \frac{d\mathcal{L}}{4\pi} \int_0^{l(\mathcal{L})} \int_0^r \varphi(x)dx\,dr, \tag{22}$$

there $l(\mathcal{L})$ is length of chord produced by intersection of straight line $\mathcal{L}$ with convex body $B$. In fact, Eq. (22) is an analogue of a standard expression used for derivation of Dirac chord method [3, Eq. (1.5)].

In such a case we have double integral along a chord due to the additional integration on source of ray

$$I^{(2)}_\varphi(l) = \int_0^l \int_0^r \varphi(x)dx\,dr \tag{23}$$

For nonconvex body and chords intersecting body on few intervals it is necessary to consider only integration on "source" point $r$ and "target" point $r_2 = r + x$ inside of these intervals. Using rather technical calculation [15] it is possible to obtain instead of Eq. (23) more difficult expression with taking into account all couples of $n$ intervals $[x_{2k}, x_{2k+1}]$, $k = 0, \dots n-1$

$$\begin{aligned} I^{(2)}_\varphi(x_{0,\dots,2n-1}) &= \sum_{k=0}^{n-1} I^{(2)}_\varphi(x_{2k+1} - x_{2k}) \\ &+ \sum_{k=1}^{n-1}\sum_{j=0}^{k-1}[I^{(2)}_\varphi(x_{2k+1} - x_{2j}) + I^{(2)}_\varphi(x_{2k} - x_{2j+1})] \\ &- \sum_{k=1}^{n-1}\sum_{j=0}^{k-1}[I^{(2)}_\varphi(x_{2k+1} - x_{2j+1}) + I^{(2)}_\varphi(x_{2k} - x_{2j})]. \end{aligned} \tag{24}$$

It includes all $n(2n-1)$ possible ordered pairs of $x_k$, $k = 0, \dots, 2n-1$ and may be rewritten

$$I^{(2)}_\varphi(x_{0,\dots,2n-1}) = \sum_{k=1}^{2n-1}\sum_{j=0}^{k-1}(-1)^{k-j+1} I^{(2)}_\varphi(x_k - x_j). \tag{25}$$

For example with two intervals there are six terms Fig. 3

$$\begin{aligned} I^{(2)}_\varphi(x_{0,\dots,3}) &= I^{(2)}_\varphi(x_1 - x_0) + I^{(2)}_\varphi(x_3 - x_2) \\ &+ I^{(2)}_\varphi(x_3 - x_0) + I^{(2)}_\varphi(x_2 - x_1) - I^{(2)}_\varphi(x_2 - x_0) - I^{(2)}_\varphi(x_3 - x_1) \end{aligned}$$

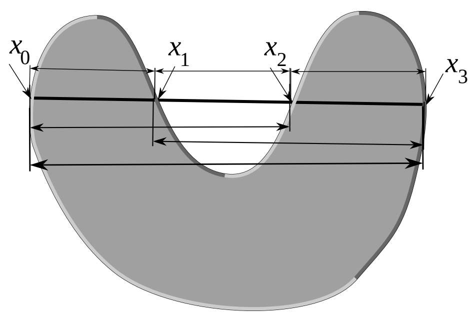


Figure 3: Chord in nonconvex body and six possible segments

Let us rewrite integral Eq. (22)

$$\mathfrak{D}_B(\varphi) = \int \frac{d\mathcal{L}}{4\pi} I^{(2)}_\varphi(\mathcal{L}), \tag{26}$$

where for convex body due to Eq. (23) $I^{(2)}_\varphi(\mathcal{L}) = I^{(2)}_\varphi(l_\mathcal{L})$. The same expression also may be used for nonconvex body if to denote $I^{(2)}_\varphi(\mathcal{L}) = I^{(2)}_\varphi(x^\mathcal{L}_{0,\ldots,2n-1})$, where $x^\mathcal{L}_0, \ldots, x^\mathcal{L}_{2n-1}$ denote all intersections of line $\mathcal{L}$ with the boundary of $B$.

On the other hand, $I^{(2)}_\varphi(\mathcal{L})$ may be expressed as a sum Eq. (25) with all possible (ordered) pair of points. It is possible to rewrite Eq. (26) for nonconvex case

$$\mathfrak{D}_B(\varphi) = \int \frac{d\mathcal{L}}{4\pi} \sum_{k=1}^{2n-1} \sum_{j=0}^{k-1} (-1)^{k-j+1} I^{(2)}_\varphi(x^\mathcal{L}_k - x^\mathcal{L}_j). \tag{27}$$

The situation is similar with expressions for rays in nonconvex body Eq. (6) and Eq. (7). Let us denote $\mu_{jk}(l)$ lengths distributions $l_{jk} = x^\mathcal{L}_k - x^\mathcal{L}_j$ produced by $n(2n-1)$ segments $(x^\mathcal{L}_j, x^\mathcal{L}_k)$ of a line $\mathcal{L}$.

If to introduce

$$\tilde{\mu}_{tot}(l) = \sum_{k=1}^{2n-1} \sum_{j=0}^{k-1} (-1)^{k-j+1} \mu_{jk}(l), \quad \tilde{\mu} = \tilde{m}^{-1} \tilde{\mu}_{tot}(l) \tag{28}$$

there $\tilde{m}$ is normalization

$$\tilde{m} = \int_0^\infty \tilde{\mu}_{tot}(l) dl. \tag{29}$$

It is possible now to write an analogue of Eq. (2) for nonconvex body

$$\mathfrak{D}_B(\varphi) = \tilde{s}_B \int_0^\infty \tilde{\mu}(l) I^{(2)}_\varphi(l) dl = \tilde{s}_B \int_0^\infty \tilde{\mu}(l) \Big( \int_0^l \int_0^r \varphi(x) dx\, dr \Big) dl, \tag{30}$$

where $\tilde{s}_B$ is some constant. For convex body $\tilde{s}_B = S_B/4$

For convex body $\tilde{\mu}(l) = \mu(l)$ and Eq. (30) may be explained using idea of averaging and mathematical expectation Eq. (17) already discussed for DD and RLD. Let us consider average of function $f(\mathcal{L}) = I^{(2)}_\varphi(l_\mathcal{L})$ on four-dimensional set $\mathcal{L}[B]$ of all straight lines intersecting body $B$.

$$\frac{1}{w_B} \int_{\mathcal{L}[B]} I^{(2)}_\varphi(l_\mathcal{L}) d\mathcal{L} = \int_0^\infty I^{(2)}_\varphi(l) \mu(l) dl, \tag{31}$$

where $w_B$ is measure (4D volume) of $\mathcal{L}[B]$. For convex body it may be expressed as $w_B = \pi S_B$ due to Cauchy relationship [15, 20, 21, 22, 24, 25] and after comparison of Eq. (31) and Eq. (22) we obtain necessary coefficient $w_B/(4\pi) = S_B/4$ used in Eq. (2).

For nonconvex body there are $n(2n-1)$ distributions $\mu_{jk}(l)$ instead of one and Eq. (30) is obtained via alternating sum Eq. (27) of this distributions and so here is $\tilde{s}_B = \tilde{m}_B^{-1} w_B/(4\pi)$ with $w_B$ is a measure for a set of all straight lines intersecting $B$ and $\tilde{m}_B^{-1}$ is constant used in definition of $\tilde{\mu}(l)$ Eq. (28). The problem here is absence of simple methods of calculation $w_B$ and $\tilde{m}_B$ for nonconvex body and so it may be convenient to consider yet another approach for finding $\tilde{s}_B$.

It is possible to use analogue of relation Eq. (11). Integration by parts of Eq. (7) for nonconvex body produces

$$\mathfrak{D}_B(\varphi) = V_B \int_0^\infty [-\tilde{\imath}'(l)] \Big( \int_0^l \int_0^r \varphi(x) dx\, dr \Big) dl \tag{32}$$

and after comparison with Eq. (30) it is possible to write

$$\begin{aligned} -V_B \tilde{\imath}'(l) &= \tilde{s}_B \tilde{\mu}(l) \\ -V_B \int_0^\infty l\, \tilde{\imath}'(l) dl &= \tilde{s}_B \int_0^\infty l\, \tilde{\mu}(l) dl \\ V_B \int_0^\infty \tilde{\imath}(l) dl &= \tilde{s}_B \bar{l} \int_0^\infty \tilde{\mu}(l) dl, \end{aligned}$$

where by definition $\bar{l}_B = \int l \tilde{\mu}_B(l) / \int \tilde{\mu}_B(l)$ and due to normalization condition for $\tilde{\imath}(l)$ and $\tilde{\mu}(l)$

$$\tilde{s}_B = V_B / \bar{l}_B. \tag{33}$$

For convex body $\bar{l}_B$ is average chord length. For nonconvex body it is equal to average chord length for multi-chord distribution (MCD) mentioned earlier, because sums of lengths of all intervals in two last terms of Eq. (24) compensate each other. It is clarified below in Sec. 4.2 about Monte Carlo simulation.

In fact, the Cauchy relationship Eq. (14) for average chord length for MCD is proved for broad class of nonconvex bodies [7] and so it is also possible to write due to Eq. (33) in such a case

$$\tilde{s}_B = S_B / 4. \tag{34}$$

In numerical methods using Eq. (33) with $\bar{l}_B$ sometimes may be preferable. It is instructive to consider an example with so-called voxel presentation of a body as a decomposition on small cubes or parallelepipeds. In such a case surface is not smooth and problem with correct approximation of surface area may not be resolved even for a formal limiting case with cubes of arbitrary small dimensions, *e.g.* for a sphere such a limit is $6\pi r^2$ instead of $4\pi r^2$.

## 4.2 Method Monte Carlo with chords

Let us consider some questions of Monte Carlo generation of quasi-probability distribution $\tilde{\mu}(l)$. For each straight lines with $n > 1$ intervals inside a body $B$ it is necessary to consider $2n$ points of intersection with the boundary of $B$. Tangent points should be counted twice, but such degenerated cases are not considered here for simplicity. Let us mark the points by numbers $x_k$, $k = 0, \ldots, 2n-1$, there $x_0 = 0$ and other $x_k$ denote distances along given straight line, *i.e.* $x_k = |\mathbf{r}_k - \mathbf{r}_0|$ there $\mathbf{r}_k$ are positions of points of intersections in three-dimensional space.

It is clear from further consideration, that it is possible to use opposite order of points $\mathbf{r}_k \leftrightarrow \mathbf{r}_{2n-k-1}$ and so direction of a line does not matter. Anyway, in real calculations it is often used *directed lines*. Standard algorithms of generation of uniform isotropic set of straight lines should be discussed elsewhere.

Let us discuss procedure of construction of $\tilde{\mu}(l)$ for given line. If line intersects body $n$ times, it is necessary to consider set of $2n$ numbers $x_k$ defined above and calculate lengths $l_{jk} = (x_k - x_j)$ for all $k > j$, *i.e.* $j = 0, \dots, k-1$ for each $k = 1, \dots, 2n-1$.

For given $l_{jk}$ number in relevant bin should be *increased* by unit for *odd* $k - j$ and *decreased* by unit otherwise, *i.e* if $k - j$ is *even*. For $2n$ indexes there are $1 + 2 + \cdots + (2n-1) = n(2n-1)$ ordered pairs. Between them $n$ pairs $(x_{2k}, x_{2k+1})$, $k = 0, \dots, n-1$ represent usual chords inside body and have positive contributions.

Remaining $n(2n-2)$ pairs are not corresponding to continuous intervals inside body and may be divided on two equal groups. There are $n(n-1)$ pairs with positive contribution, *i.e.* $(x_{2j}, x_{2k+1})$ or $(x_{2j+1}, x_{2k})$ with $k = 1, \dots, n-1$ and $j = 0, \dots, k-1$. For other $n(n-1)$ pairs, *i.e.* $(x_{2j}, x_{2k})$ or $(x_{2j+1}, x_{2k+1})$ with $k = 1, \dots, n-1$ and $j = 0, \dots, k-1$, numbers in bins should be decreased.

It is clear also from such representation, that sums of lengths of the pairs in two last groups compensate each other, because

$$(x_{2k+1} - x_{2j}) + (x_{2k} - x_{2j+1}) = (x_{2k} - x_{2j}) + (x_{2k+1} - x_{2j+1}).$$

So total contribution to length is equivalent with sum of $n$ chords inside body.

There is also additional subtlety with normalization. For each straight line the total increase of values in all affected bins is

$$\Delta N_{tot} = n + n(n-1) - n(n-1) = n.$$

So two different counters are relevant for a simulation: number of lines $N_l$ and sum of numbers in all bins $N_{tot} \ge N_l$.

For normalization the (quasi)distribution should be divided on $N_{tot}$. It is similar with MCD distribution, then for some lines there are $n > 1$ chords and for such a case $N_{tot}$ corresponds to total number of all chords.

It was shown above, that total sum of all lengths with taking into account signs is equal with sum of $n$ chords. But the normalization is the same as for MCD case and so average value of length for quasi-probability distribution constructed here is the same as for MCD distribution that could be produced from the same simulation. In a limit $N_l \to \infty$ it produces equality for $\bar{l}$ already mentioned and used above in Eq. (34).

Total number of lines $N_l$ corresponds to normalization for OCD case, then for each line is considered one “aggregated” chord equivalent to union of all $n$ intervals inside body. It is also related with measure of set of all straight lines intersecting considered body. Earlier in Eq. (31) this measure was denoted as $w_B$.

Yet another application of both $N_{tot}$ and $N_l$ is calculation of a constant $\tilde{m}$ used earlier in Eq. (28). It may be expressed via relation between $\tilde{\mu}_{tot}$ (that is not normalized on unit due to contribution of lines intersecting body more than one time) and $\tilde{\mu}$. So $\tilde{m}$ is limit of ratio between total number of chords $N_{tot}$ (*cf* MCD) and total number of straight lines $N_l$ (*cf* OCD)

$$\tilde{m} = \lim_{N_l \to \infty} N_{tot}/N_l. \tag{35}$$

# 5 Multi-body case

## 5.1 Some equations with two different bodies

Let us return to initial question of calculation of integral Eq. (1) with two different bodies. Here is also convenient to consider simple model with particles moving along straight lines in homogeneous isotropic media and to use interpretation of Eq. (1) as a fraction of energy emitted in $B_1$ and absorbed in $B_2$.

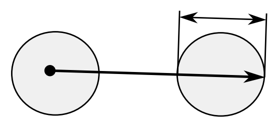

Figure 4: Ray from $B_1$ with interval inside $B_2$

Let us consider a particle emitted in the first body with straight trajectory intersecting the second one Fig. 4. If the law of absorption is the same in both bodies and environment between them, it is possible to describe amount of energy absorbed in second body as

$$\int_a^b \varphi(x)dx = I_\varphi(b) - I_\varphi(a), \tag{36}$$

where $a$ and $b$ are distances from source to two intersections of second body by ray and $I_\varphi$ is defined above in Eq. (4).

More direct way of calculation for convex $B_2$ Eq. (1) is to write analogue of Eq. (8)

$$\mathfrak{F}_{B_1}^{B_2}(\varphi) = \int_{B_1} d\mathbf{V}_1 \int_{\theta_{\min}(\mathbf{r}_1,\phi)}^{\theta_{\max}(\mathbf{r}_1,\phi)} \sin\theta d\theta \int_{\phi_{\min}(\mathbf{r}_1)}^{\phi_{\max}(\mathbf{r}_1)} d\phi \int_{a(\mathbf{r}_1,\theta,\phi)}^{b(\mathbf{r}_1,\theta,\phi)} \frac{\varphi(R)}{4\pi} dR, \tag{37}$$

where $\theta_{\min}, \theta_{\max}, \phi_{\min}, \phi_{\max}$ describe angular limits of integrations for given point $\mathbf{r}_1$ and $a$, $b$ is radial distances for given point and direction. It may be simpler to use an analogue of Eq. (9)

$$\mathfrak{F}_{B_1}^{B_2}(\varphi) = \int_{B_1} d\mathbf{V}_1 \int_{\mathbf{S}(\mathbf{r_1},B_2)} \frac{d\mathbf{\Omega}}{4\pi} \int_{a(\mathbf{r}_1,\mathbf{\Omega})}^{b(\mathbf{r}_1,\mathbf{\Omega})} \varphi(R)dR, \tag{38}$$

where $\mathbf{S}(\mathbf{r_1}, B_2)$ is central projection from point $\mathbf{r_1}$ of body $B_2$ to surface of unit sphere.

## 5.2 Relation with methods for single body

For two nonconvex bodies expressions may be even more difficult, but it is possible to use general principle to adapt already developed approach with single body [16]. Let us consider both bodies as sources and consider four integrals $\mathfrak{F}_{B_j}^{B_k}(\varphi)$, $j = 1, 2$, $k = 1, 2$, *i.e.* $\mathfrak{F}_{B_1}^{B_1} = \mathfrak{D}_{B_1}$, $\mathfrak{F}_{B_2}^{B_2} = \mathfrak{D}_{B_2}$, $\mathfrak{F}_{B_1}^{B_2} = \mathfrak{F}_{B_2}^{B_1}$. Each integral take into account only particles emitted in $B_j$ and absorbed in $B_k$.

The double integrals Eq. (1) and Eq. (2) comply with simple relations

$$\mathfrak{D}_{B_1 \cup B_2}(\varphi) = \mathfrak{F}_{B_1}^{B_1}(\varphi) + \mathfrak{F}_{B_1}^{B_2}(\varphi) + \mathfrak{F}_{B_2}^{B_1}(\varphi) + \mathfrak{F}_{B_2}^{B_2}(\varphi) \tag{39}$$

and

$$2\mathfrak{F}_{B_1}^{B_2}(\varphi) = \mathfrak{D}_{B_1 \cup B_2}(\varphi) - \mathfrak{D}_{B_1}(\varphi) - \mathfrak{D}_{B_2}(\varphi). \tag{40}$$

So many equations with two bodies may be reduced to already discussed case of single body using union of these bodies $B = B_1 \cup B_2$.

Here is suggested, that $B_1$ does not intersect $B_2$. For overlapping bodies it should be taken into account decomposition on three parts: $B_1 \cup B_2$, $B_1 \setminus B_2$ and $B_2 \setminus B_1$. Instead of Eq. (40) in such a case it may be used modified expression

$$2\mathfrak{F}_{B_1}^{B_2}(\varphi) = \mathfrak{D}_{B_1 \cup B_2}(\varphi) + \mathfrak{D}_{B_1 \cap B_2}(\varphi) - \mathfrak{D}_{B_1}(\varphi) - \mathfrak{D}_{B_2}(\varphi). \tag{41}$$

Due to such equations numerical methods discussed above let us find Eq. (1) after separate calculation of three or four terms in Eq. (40) or Eq. (41). However, more direct methods discussed further are also useful and may be simply generalized for case with many bodies.

For simpler case of two *disjoint bodies* it is possible to use almost straightforward modifications of Monte Carlo algorithms discussed above [16]. Here Eq. (39) may be even more convenient for explanation than Eq. (40), because it demonstrates, that distributions obtained in simulation may be divided on four parts (for each pair source-target) without significant modification of algorithms for general nonconvex body discussed above.

## 5.3 Application to calculations with rays

For sampling with rays are used source points distributed in both bodies with equivalent density. All intersections of a ray in both bodies are checked and appropriate bins are changed in four histograms $H_{jk}(l)$ marked by indexes source-target.

Joint consideration of all distributions let to tackle a problem with normalization. For the function $\tilde{\imath}$ term "quasi-probability distribution" could be justified due to unit normalization and some relation with probability density for lengths of rays in convex body, but if to write an analogue of Eq. (3) for the integral Eq. (1)

$$\mathfrak{F}_{B_1}^{B_2}(\varphi) = W_{12} \int_0^\infty \tilde{\imath}_{(12)}(l) \Big( \int_0^l \varphi(x) dx \Big) dl, \tag{42}$$

where $W_{12}$ is an unknown constant, it becomes clear that $\tilde{\iota}_{(12)}(l)$ may not be normalized for disjoint bodies, because due to Eq. (40)

$$W_{12} \int_0^\infty \tilde{\iota}_{(12)}(l)dl = (V_1 + V_2) \int \tilde{\iota}_\cup(l)dl - V_1 \int \tilde{\iota}_1(l)dl - V_2 \int \tilde{\iota}_2(l)dl = 0$$

where integrals of all functions $\tilde{\iota}_1(l)$, $\tilde{\iota}_2(l)$ and $\tilde{\iota}_\cup(l) = \tilde{\iota}_{B_1 \cup B_2}(l)$ are normalized on unit.

However, if to include all four densities as components in the single process described by quasi-probability distribution, introduced earlier

$$\tilde{\iota}_\cup(l) = \sum_{jk} \tilde{\iota}_{(jk)}(l), \tag{43}$$

it is possible to consider $\tilde{\iota}_{(jk)}(l)$ as elements of the same matrix $\tilde{\iota}(l)$ with the common normalization. The same approach may be used for more than two bodies.

### 5.4 Application to calculations with chords

For expression of Eq. (1) using chords distributions also may be used similar principles [16]. Here is also appropriate to use Eq. (39). It is considered for a straight line $2n$ intersections $x_0, \ldots, x_{2n-1}$, there boundaries of both bodies are taken into account. Each intersection should be marked by additional index $x_l^j$, where $j = 1, 2$ for $B_1$, $B_2$.

Each segment $(x_l^j, x_m^k)$ already has two additional indexes $j$ and $k$ representing for two bodies four possible combinations and it produces distributions $\tilde{\mu}_{(jk)}$, $k, j = 1, 2$. It only should be mentioned that due to symmetry for chords "source" and "target" body are hardly could be distinguished. Due to such property it is reasonable to use only three separate histograms $H_{11}$, $H_{22}$ and $H_{12} + H_{21}$ and to define $\tilde{\mu}_{\{jk\}}(l)$ as a symmetric matrix.

It may be directly generalized for a case with $m$ bodies with $k, j = 1, \ldots, m$. Advantages of application of discussed method may be illustrated by consideration of domain with many different bodies intersected by set of straight lines. It is possible to calculate all $m^2$ integrals $\mathfrak{F}_{B_j}^{B_k}$ during the same Monte Carlo simulation.

Here only $m(m-1)/2$ integrals are different due to symmetry, but it is anyway may be a big number. For medical applications with $15 - 20$ objects (organs) it is calculation of hundreds values in single Monte Carlo simulation. In fact, speed up may be even more significant due to possibility to split each body on few zones. Such subdivision may be necessary for taking into account different intensity of emitters in the different parts of some objects.

There is only one subtlety for calculation with few zones: it is necessary to split formally each surface between two zones on two coinciding boundaries. In such a case all equations above are valid, but there are some intervals with zero length. Such intervals may be simply omitted, because integration along them produces zero value.

## 5.5 Analytical expressions for two bodies

There are useful analogues of expressions discussed in Sec. 3 for the case with two bodies. Function $\eta_{(12)}(l)$ may be defined as a probability density of distance between pair of points homogeneously distributed in first and second body respectively. Analytical expressions written below may be used for testing of Monte Carlo simulation and some clarification. Technical details may be found in [16].

The correlation function $\gamma_{(12)}(l)$ is defined for two bodies with unit densities $\rho_k(\mathbf{r}) = 1$ for $\mathbf{r} \in B_k$, $k = 1, 2$ as

$$\gamma_{(12)}(\mathbf{r}) = \int_{B_1} \rho_1(\mathbf{r}_1)\rho_2(\mathbf{r}_1 + \mathbf{r})d\mathbf{V}_1, \quad \gamma_{(12)}(l) = \frac{1}{4\pi l^2}\int_{|\mathbf{r}|=l} \gamma(\mathbf{r})d\mathbf{\Omega}. \tag{44}$$

It is possible to derive direct analogue of Eq. (13)

$$\eta_{(12)} = \frac{4\pi l^2}{V_1 V_2}\gamma_{(12)}(l) \tag{45}$$

and generalisation of Eq. (18)

$$\mathfrak{F}_{B_1}^{B_2}(\varphi) = \int_0^\infty \varphi(l)\,\gamma_{(12)}(l)dl. \tag{46}$$

Using integrations of Eq. (46) by parts it is possible to to express $\tilde{\iota}_{(12)}$ and $\tilde{\mu}_{(12)}$ as first and second derivatives of correlation function $\gamma_{(12)}(l)$ respectively. It is similar with Eq. (12) and Eq. (10). If to use normalization on union of bodies suggested above and Cauchy equation for average chord length, it may be written

$$\tilde{\mu}_{(12)}(l) = \frac{4}{S_{B_1} + S_{B_2}}\gamma''_{(12)}(l), \tag{47}$$

$$\tilde{\iota}_{(12)}(l) = -\frac{1}{V_{B_1} + V_{B_2}}\gamma'_{(12)}(l). \tag{48}$$

So, in already mentioned expression for rays Eq. (42) for normalization on union of two bodies instead of “unknown constant” should be used

$$W_{12} = V_{B_1} + V_{B_2} \tag{49}$$

and the generalization of the Dirac chord method for calculation of Eq. (1) may be expressed formally as

$$\mathfrak{F}_{B_1}^{B_2}(\varphi) = \frac{S_{B_1} + S_{B_2}}{4}\int_0^\infty \tilde{\mu}_{(12)}(l)\Big(\int_0^l\int_0^r \varphi(x)dx\,dr\Big)dl. \tag{50}$$

## 6 Conclusion

In this paper is discussed new approach with application of quasi-probability distributions (signed measures) to calculations of integrals Eq. (1) and Eq. (2) useful in many areas of physics. It is written with a purpose to present a fairly brief, but closed description of considered methods. Additional technical details, proofs of some equations together with appropriate links with theory of geometrical probabilities may be found elsewhere [15, 16].

It is shown, how models with ray and chord length distributions suitable for a single convex body should be altered for nonconvex bodies and multi-body systems. Essential new property of such extensions is necessity to use instead of probability densities some functions which sometimes are not satisfying non-negativity condition.

Maybe such a counterintuitive "negative probability" produced certain difficulty and delay of development and application of this methods despite of high effectiveness of numerical algorithms based on ray and chord distributions. On the other hand, such quasi-probability distributions are rather common in quantum physics due to so-called Wigner function representation [26] and Feynman even wrote an essay about concept of negative probability with reasonable examples both in quantum and classical physics [27].

In fact, the functions $\tilde{\iota}(l)$ and $\tilde{\mu}(l)$ do not necessary *directly* related with probability distributions and so should not cause some conceptual challenges. Appearance of negative values may be simply illustrated using Eq. (5) and Fig. 1. Here ray $(0, l_3)$ includes ray $(0, l_1)$ already taken into account and interval $(l_1, l_2)$ outside of the body, that should not be counted at all.

Here for work with interval $(l_2, l_3)$ we have to use expressions like Eq. (5), but it may be described in standard probability theory. It is known probability measures for sets $R_1 = A$, $R_2 = A \cup B$, $R_3 = A \cup B \cup C$ and it is possible to write for probability measure of $C$ $\mathbf{P}(C) = \mathbf{P}(R_3 \setminus R_2) = \mathbf{P}(R_3) - \mathbf{P}(R_2)$ (*cf* constructions of $\sigma$-algebra of events [23]).

In construction of $\tilde{\iota(l)}$ are used overlapping sets, *i.e.* rays with the same origin Fig. 1. Positive and negative terms like $\mathbf{P}(R_3)$ and $-\mathbf{P}(R_2)$ used for calculation of the same $\mathbf{P}(C)$ affect two ranges of argument $\tilde{\iota(l)}$. So for $l = R_3$ there is some positive gain, but for $l = R_2$ there is the same decrease and it may produce negative values of $\tilde{\iota(l)}$ for some intervals of $l$. We have added an additional hit to some bin and trying to compensate that by removal from another one, but it may produce a negative result.

Construction of $\tilde{\iota(l)}$ is simpler, than generalization of chord length distribution $\tilde{\mu(l)}$, but reason of appearance of negative values in both cases are similar. Number of sets in expression for a ray grows linearly with respect to number of intersection and for chord it is quadratic dependence. Construction of sets also more difficult, but here alternating signs in expressions like Eq. (24) again corresponds to an expression with unions and differences of some overlapped sets.

# References


[1] J. K. Shultis and R. E. Faw, "Radiation shielding technology," *Health Phys.* **88(4)**, 297–322 (2005).

[2] W. S. Snyder, M.R. Ford, and G. G. Warner, "Estimates of specific absorbed fractions for photon sources uniformly distributed in various organs of a heterogeneous phantom," *MIRD Pamplet No. 5, revised* (New York, NY: Society of Nuclear Medicine, 1978).

[3] P. A. M. Dirac, "Approximate rate of neutron multiplication for a solid of arbitrary shape and uniform density, I: General theory," in *The Collected Works of P. A. M. Dirac 1924–1948*, R. H. Dalitz (ed.), 1115–1128 (Oxford University Press, Oxford, 1995).

[4] P. A. M. Dirac, K. Fuchs, R. Peierls, and P. Preston, "Approximate rate of neutron multiplication for a solid of arbitrary shape and uniform density, II: Application to the oblate spheroid, hemisphere and oblate hemispheroid," *ibid*, 1129–1145.

[5] N. Metropolis, "The beginning of the Monte Carlo method," *Los Alamos Science* **15**, 125–130 (1987).

[6] W. Gille, "Chord length distributions and small-angle scattering," *Eur. Phys. J. B* **17**, 371–383 (2000).

[7] A. Mazzolo, B. Roesslinger, and W. Gille, "Properties of chord length distributions of nonconvex bodies," *J. Math. Phys.* **44**, 6195–6208 (2003).

[8] A. Mazzolo, B. Roesslinger, and C. M. Diop, "On the properties of the chord length distribution, from integral geometry to reactor physics," *Ann. Nucl. Energy* **30**, 1391–1400 (2003).

[9] C. Burger and W. Ruland, "Analysis of chord-length distributions," *Acta Cryst.* **A57**, 482–491 (2001).

[10] N. Stribeck, "Extraction of domain structure information from small-angle scattering patterns of bulk materials," *J. Appl. Cryst.* **34**, 496–503 (2001).

[11] W. Gille, "Linear simulation models for real-space interpretation of small-angle scattering experiments of random two-phase systems," *Waves Random Media* **12**, 85–97 (2002).

[12] S. Hansen, "Estimation of chord length distributions from small-angle scattering using indirect Fourier transformation," *J. Appl. Cryst.* **36**, 1190–1196 (2003).

[13] W. Gille, A. Mazzolo, and B. Roesslinger, "Analysis of the initial slope of the small-angle scattering correlation function of a particle," *Part. Part. Syst. Charact.* **22**, 254–260 (2005).

[14] S. Torquato and B. Lu, "Chord-length distribution function for two-phase random media," *Phys. Rev. E* **47**, 2950–2953 (1993).

[15] A. Yu. Vlasov, "Signed chord length distribution. I," `arXiv:0711.4734 [math-ph]` (2007).

[16] A. Yu. Vlasov, "Signed chord length distribution. II," `arXiv:0904.3646 [math-ph]` (2009).

[17] A. N. Kolmogorov and S. V. Fomin, *Introductory real analysis*, (Dover, New York, 1975).

[18] A. M. Kellerer, "Consideration on the random traversal of convex bodies and solutions for general cylinders," *Radiat. Res.* **47**, 359–376 (1971).

[19] A. Mazzolo, "Probability density distribution of random line segments inside a convex body: Application to random media," *J. Math. Phys.* **44**, 853–863 (2003).

[20] M. G. Kendall and P. A. P. Morran, *Geometrical probability*, (Griffin, London, 1963).

[21] L. A. Santaló, *Integral geometry and geometric probability*, (Addison–Wesley, Reading, 1976).

[22] A. Cauchy, "Mémoire sur la rectivication des courbes et la quadrature des surfaces courbes," *Œuvres completès* **T. 2**, 167–177, (Gauthier-Villars, Paris, 1908).

[23] A. Skorokhod and I. Prokhorov, *Basic principles and applications of probability theory*, (Springer, Berlin, 2005).

[24] G. Matheron, *Random sets and integral geometry*, (Wiley, New York, 1975).

[25] S. Helgason, *Groups and geometric analysis*, (Academic Press, New York, 1984).

[26] E. Wigner, "On the Quantum Correction For Thermodynamic Equilibrium," *Phys. Rev.* **40**, 749 – 759 (1932).

[27] R. P. Feynman, "Negative probability," in *Quantum implications: Essays in honor of David Bohm*, edited by B. J. Hiley and F. D. Peat (Routledge and Kegan Paul, London, 1987), Chap. 13, pp 235–248.